Experimental Validation of an Identification Procedure of PEMFC Stack State of Health Using EIS Combined with a Physical Impedance Modelling

Stéphane Chevalier*[a,b] , Christophe Josset[b], Jean-Christophe Olivier[a], Bruno Auvity[b], Didier Trichet[a], Mohamed Machmoum[a]

[a] Institut de Recherche en Energie Electrique de Nantes Atlantique (EA 4642), 37 boulevard de l'université, 44602 Saint-Nazaire, France
[b] Laboratoire de Thermocinétique de Nantes (CNR UMR 6607), rue Christian Pauc 44306 Nantes, France
stephane.chevalier@univ-nantes.fr

An original modelling of PEM fuel cell impedance is developed in our laboratory. It is based on the 1D resolution in the frequency domain of the physical equations taken into account the main phenomena encountered in PEM fuel cell: electrochemical reactions, ionic transport, charge and mass transfer in cathode electrode and GDL. In the present work, the impedance model has been validated on experimental impedance measurements run on 16 cells stack (400 W maximum electrical output) where every cell impedances have been recorded simultaneously. Coupled with a dynamic physical model an accurate stack characterisation has been performed over a relative large current density range from 0.08 A/cm^2 to 0.6 A/cm^2.

1. Introduction

Electrochemical Impedance Spectroscopy (E.I.S.) is now widely used by the scientific community to characterise and diagnose the PEM fuel cell state of health.(Yuan et al. 2007). Most of researches are focused on single cell experiments where the cell global behaviour is studied under different operating conditions i.e. gas stoichiometry, temperature, humidity... Through these studies, the high impact of water on cell performances has been identified and it is admitted that optimal conditions are reached when enough water inside the membrane is present to conduct protons from anode to cathode. But too much water in the cell may also lead to gas diffusion pores filling with a risk of cell degradations (Schmittinger and Vahidi 2008). Thus, the issue is to find the optimal water management to avoid both drying and flooding conditions. Finally, recent results shown by Gerteisen et al. (Gerteisen et al. 2011) have recently obtained impedance spectra of a 7 by 7 segmented cells, using a 50 channels frequency analyser. It has been reported that even at high working potential, inhomogeneous current densities are presents through the cell active area, mainly link to an insufficient water management.

Concerning fuel cell stack, only few experimentations have been reported through the literature. Fouquet et al. (Fouquet et al., 2006) and Rodat et al. (Rodat et al., 2009) have recently published very interesting results on stack diagnostic. They have used the so-called Randles circuit model to build a diagnostic tool. They have been able to identify the optimal operating conditions or to detect degradation scenarios like stack flooding or drying. Nevertheless, they performed E.I.S. measurements on the entire stack, or on one single cell in the stack without recording every cell impedance. This lack of data may lead to wrong diagnostic. Indeed, it is known that high thermal gradients present through the stack can lead to different cell degradation scenarios. For example, at the stack extremities (inlet and outlet) where the temperature is generally lower, cells tend to flood, contrary to the stack centre which is generally a drying area. Thus, to perform an accurate stack diagnostic, each cell state of health has to be recorded. Moreover, the diagnostic conclusion is limited to the explored operating conditions. Indeed, the Randle circuit model impose a heavy experimental procedure: Fouquet et al. have performed more than 150 impedance

records. Each cell parameter, i.e. membrane resistance, polarisation resistance..., is identified for only one operating condition and/or working point.

In this paper, we report experimental results performed on a 16 cells stack (active area of 60 cm²) where each cell impedances are recorded simultaneously over different operating currents. Cells characterization is done using a physical model based on the fundamental fuel cell equations (Fick law, Ohm law and Tafel law) rather than with Randle model or parametric model as proposed by (Ziogou et al., 2010). This model allows the identification of the limiting processes, and the evaluation of the cell state of health over different working conditions with restricted parameters set, i.e. at different stack currents. This new experimental results come to validate the numerical procedure of cell failure identification developed by (Chevalier et al., 2013).

2. Experimental setup

2.1 Stack test station description

The fuel cell stack used in the experiments is composed of 16 PEM cells provided by the Swiss company MES SA, for a 400 W electrical power output. Contrary to the usual fuel cell technology, these kind of cells run under low temperature conditions, typically 40 °C, and with very high air stoichiometry (Buaud et al. 2008), mainly due to the parallel channels configuration on the cathode side. Indeed, this channel design is highly sensitive to clogging, thus high air flow rate is needed to avoid cell flooding. Stack temperature is regulated by air forced convection between each cells with two fans.

The stack is connected to a gas conditioning bench, as depicted on Figure 1. Both reactants air and hydrogen are controlled in temperature, hygrometry, flow rate and pressure. Volumetric flow controllers are used on a range of 1-110 Ln/min (air) and 0.1-10 Ln/min (hydrogen), and the relative pressure can be regulated between 0 and 4 bar. Reactants hygrometry is set imposing the gas temperature and water mass flow injected trough the vaporizers, then the gas temperature is kept constant up to the stack inlets. With a 40°C stack temperature the air relative humidity can be set from 0% to 100%.

Impedance spectra and stack voltages are recorded by 50 parallel channels spectrometer analyser provided the Material Mates society, see (Gerteisen et al. 2011). The stack is directly connected to the electronic load. Cell voltages are recorded as well as their electrochemical impedance on the range of 10 kHz to 0.1 Hz. The sinusoidal peak to peak amplitude current is imposed to 10% of the fuel cell DC current. Twelve thermocouples have been inserted through the stack in order to estimate the temperature profile of the stack. The stack temperature is considered as the mean value of these 12 thermocouples.
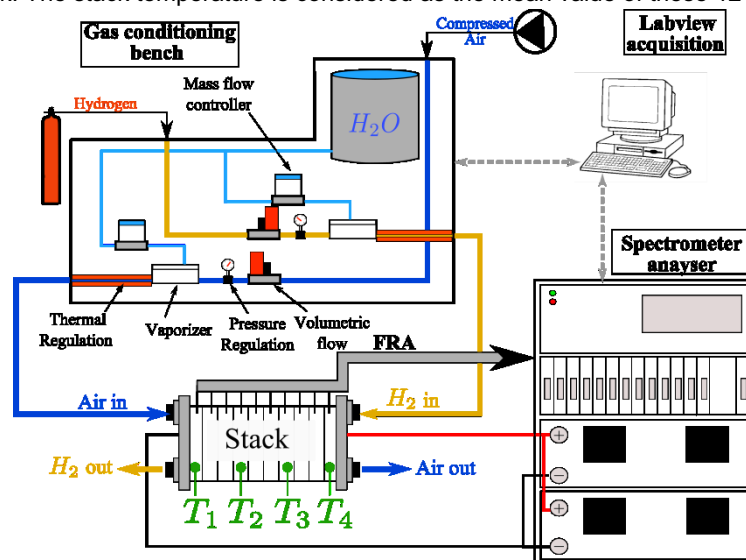

Figure 1: Scheme of the experimental setup used to characterise the fuel cell stack. It is composed of a gas conditioning bench, a temperature acquisition system and a spectrometer analyser

2.2 Stack impedance measurements

Measurements are carried out under the experimental conditions given Table 1. Five operating between 5A and 35A have been recorded under constant stoichiometry conditions where each cell impedance responses have been measured independently. The stack temperature is set to 40 °C. Results are summarized in Nyquist plot through the Figure 2.

As expected, the cell impedance decreases from low current 5A to high current 35A. The cell membrane resistance decreasing can also be pointed out on each cell. As it is generally admitted, the current production allows a higher membrane humidification due to the water created in the catalyst layer thus decreasing the ohmic resistance.. An homogeneous behaviour of the cells through the stack can be observed. Nevertheless, few differences can be noted, particularly with the cell number 15. To understand and identify the phenomenon linked to these performances limitations, a dynamic PEM fuel cell modelling is developed in section 3.
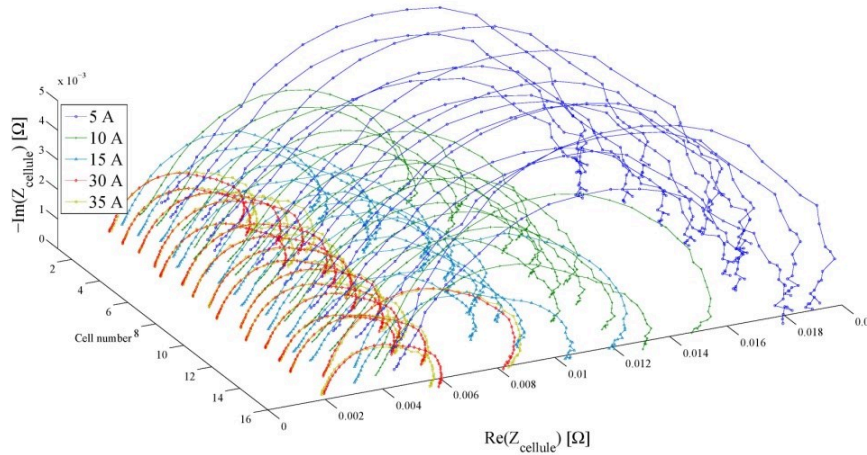

Figure 2: Nyquist plot of stack cells impedances. They have been recorded at 10, 15 and 20 A

Table 1: Experimental conditions

Description	Anode (hydrogen)	Cathode (Air)
Temperature (°C)	40	40
Reactant relative humidity (%)	0	50
Reactant absolute pressure (bar)	1.5	1
Reactant stoichiometry (-)	2	8

3. Numerical model

Each cell impedance response is analysed using a numerical model mainly based on the theory developed first by Springer et al. (Springer 1996) then by Eikerling et al. (Eikerling and Kornyshev 1999). This kind of model allows a fine description of the electrochemical transfer through a PEM fuel cell, each losses i.e. gas depletions, membrane resistance degradations, catalyst corrosion, etc. can be clearly identified. On other hand, these kind of modelling are able to reproduce the cell dynamic behaviour at different voltage/current operating point with restricted parameters set: Springer et al. used only 7 parameters to characterise their cell impedance responses on a cell voltage range from 0.81 V to 0.48 V. Thus, this approach takes advantage of reducing the experimental stack characterisation procedure because few parameters are evaluated, contrary to the equivalent circuit approach where cell parameters are evaluated on each operating point. In the following model, water production and transport through the cell won't be computed, but its impact on performances may be highlighted through its material properties like the exchange current or membrane resistance. A exchange current decreasing could be linked to a catalyst flooding or a membrane resistance increasing to a cell drying (Chevalier et al., 2013).

3.1 Cathode multiphysics a.c. and d.c. model
In the modelling only the cathode side is considered. The previous measurements (Figure 2) reveal only one kinetic loop, in the range 10-100 Hz on the impedance spectra meaning that only the cathode response plays a role. Indeed; anode kinetic loop is usually recorded in higher frequency range with specific experimental conditions involving poor anode performances, i.e. dead end mode.
The model describes ionic transport through the membrane, electrochemical processes through the electrode and gas transport through the GDL, as schemed on Figure 3. The general fuel cells equations are based on Ohm's law, Fick's law, Tafel's law and the charge and mass conservations. Through the three domains depicted on Figure 3, the electrochemical transfers and transport can be written as:

$$-\sigma_m \frac{d^2\eta_m}{dx_m^2} = 0 \tag{1}$$

$$-\sigma_e \frac{\partial^2 \eta_e}{\partial x_e^2} + \frac{C_{DL}}{L_e}\frac{\partial \eta_e}{\partial t} = -A_r i_c \frac{c_e}{c_g^{ref}}\exp\left(\frac{\eta_e}{b}\right) \tag{2}$$

$$-D_e \frac{\partial^2 c_e}{\partial x_e^2} + \frac{\partial c_e}{\partial t} = -\frac{A_r i_c}{4.F}\frac{c_e}{c_g^{ref}}\exp\left(\frac{\eta_e}{b}\right) \tag{3}$$

$$-D_g \frac{\partial^2 c_g}{\partial x_g^2} + \frac{\partial c_g}{\partial t} = 0 \tag{4}$$

Where subscripts m, e, g refer respectively to the membrane, electrode and diffusion layer domains. The two variables solved here are the over potentials η_k through the membrane and the electrode and the oxygen molar concentration c_k through the electrode and the diffusion layer. The fuel cell electrochemical properties are defined through the membrane and electrode ionic conductivities σ_e and σ_m [S/m], the electrode and GDL oxygen diffusivity coefficients D_e and D_g [m2/s], the cathode exchange current i_c [A/m2], the platinum effective area A_r [m2/m3], the double layer capacity C_{DL} [F/m2] and the Tafel slope b [V]. All this parameters are identified to fit the model on experimental measurements, see section 4. Note that all the previous equations are numerically solved using finite volume method over the electrode thickness. The non linearity of the Eq. (2-3), due to the Tafel law, needs an iterative procedure. Newton-Raphson algorithm is used to ensure solution convergence. The electrode is divided into 50 elements that satisfied the mesh convergence.
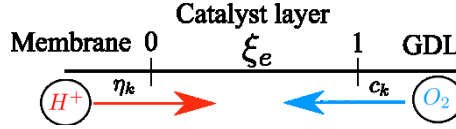

Figure 3: Membrane electrode assembly and cathode GDL scheme. ξ_e is the electrode dimensionless thickness.

3.2 States of health characterisation

The previous variables η_k and c_k in the Eq. (1-4) are decomposed in a steady and periodic part as : $\eta_e(x,t) = \eta_e{}^0(x) + \delta\eta_e(x,\omega).\exp(i.\omega.t)$. This allows two distinct resolutions :

- firstly, the model is solved in frequency domain, leading to the computation of cathode impedance (see Eq. (5)). The cell parameters may be identified by comparing the model to the cell measurements over different currents, as presented in Fig. (4).
- secondly, once the cell parameters are known the model is solved in steady states that lead to the cell potential distribution through the membrane and electrode, see Fig. 3. Thus, cell voltage losses are then deduced (Eq. 6-9) and its state of health is characterized.

$$Z_{cell}(j,\omega) = -\frac{\delta\eta_e(0,\omega)}{\delta j(\omega)} \tag{5}$$

The Fig. 4 below describes the cell voltages through the membrane electrode assembly. Ohmic losses through the membrane and the electrode can be seen due to protons flow as well as kinetic irreversibility due to the electrochemical reaction. Each voltage losses may be computed from the steady states resolution of the previous model after the parameters identification, run from the impedance measurements. Potential losses, in volt, are given by:

$$Y_{membrane} = E^{ref} - E_{cell} - \eta_e{}^0(0) \tag{6}$$

$$Y_{electrode} = \eta_e{}^0(0) - \eta_e{}^0(L_e) \tag{7}$$

$$Y_{kinetic} = \int_0^{L_e}\left(b.ln\left(\frac{c_e(x)}{c_g^{ref}}\right) + \eta_e{}^0(x)\right).dx \tag{8}$$

$$Y_{gases} = \eta_e{}^0(L_e) - Y_{kinetic} \tag{9}$$

Where L_e is the electrodes thickness given by the manufacturer. Eq. (6) to (9) are used to computed the voltages losses plotted on Fig. 7.
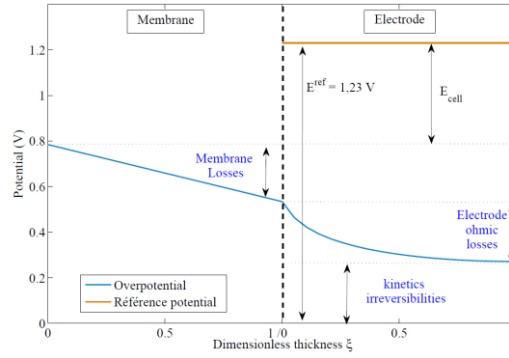
Figure 4: Scheme of overpential distribution through the membrane electrode assembly. Each cell losses may be identified and attributed to a clear phenomenon.
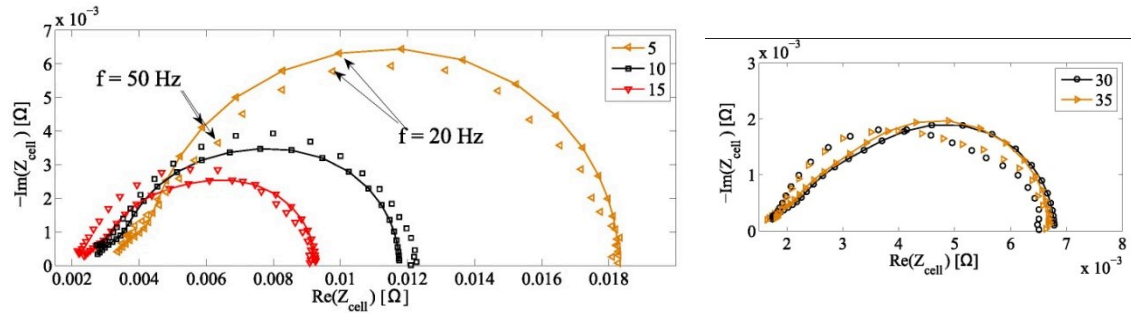
4. Fuel cell characterisation

Figure 5: Nyquist of plot cell impedance number 1. Comparison between the numerical results (solid line) and the measurements (markers) at different operating currents

Table 2: Identified model parameters from experimental data

Cell number	1	15	Mean (over the 16 cells)
Tafel slope b [V]	0.0568	0.0635	0.0552
Exchange current $A_r i_c$ [A/m^2]	5.30 10^3	5.20 10^3	5.50 10^3
Oxygen diffusivity D_g [m^2/s]	8.06 10^{-6}	7.86 10^{-6}	7.81 10^{-6}
Double layer capacity C_{DL} [F/m^2]	15.84	11.45	21.57
Reference concentration c_g^{ref} [mol/m^3]	0.0929	0.085	0.089
Membrane shape factor λ_e	0.69	0.99	0.62
GDL shape factor λ_g	24.4	29.9	21.74

To ensure a sufficient sensitivity, the parameters are identified based on a multi-spectra inversion. Hence, the optimisation algorithm looks for an unique parameters set able to reproduce the cell impedance behaviour over different operating current. The fitted parameters are summarised in Table 2 for the cell number 1 and 15, as well as the mean cell parameters; they are in the range generally admitted by the literature. Results presented in Fig. 5 show the impedance in Nyquist plot for different currents. Good agreements between the model and the measures can be observed. The fuel cell behaviour is well reproduced over the entire current range, particularly at low current (5, 10 and 15A) where the 45 ° slope is well reproduced by the model at high frequency. Nevertheless, a deviation on the kinetic loop is seen when the current increase (30 and 35 A). The electrochemical transfer description through the electrode may be improved to obtain a better fit of the cell kinetic loop and to enhance the exactness of the parameter value identified.

From the parameters given in Table 2, the voltage losses are computed and presented in Fig. 6. As it has been highlighted, the cell 15 presents an higher impedance responses than the others cells. Thanks to our model, it can be pointed out that the cell 15 reports higher voltages losses through its membrane and the

electrochemical reaction. This latter is particularly pronounced under low currents. However, few losses are attributed to the gasses, it can be concluded that this cell is sufficiently fed as well as the other cells.

Based on these observations, it may be concluded that all the total cell current should be produced in a restrictive area of the cell that induced higher kinetic losses. Thus, the other part of the cell is less humidified (because less current is locally produced), so the membrane gets locally a higher resistance, as seen on cell 15 spectra on Fig 2. Finally it can be concluded that the origin of this degradation may comes from a local lack of platinum through the catalyst layer.
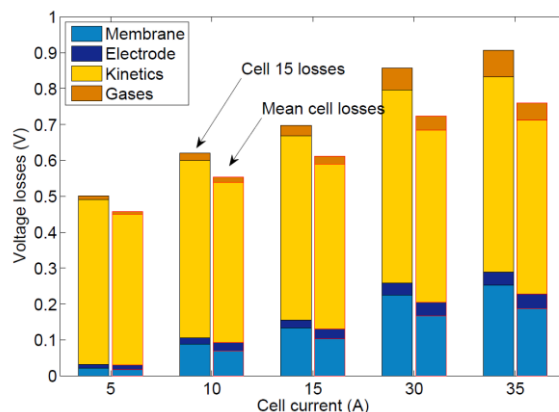

Figure 6: Histogram of voltage losses at different currents. Comparison between the cell number 15 and the mean cell voltage losses.

5. Conclusion

Fuel cell impedance measurements are clearly a promising way to characterize and identify the fuel cell state of health when coupled with the appropriate physical fuel cell model. It has been shown that even if the large majority of 16 cells stack run with similar performances, simultaneous individual cell impedance measurements constitute an accurate diagnostic method to detect an even slightly degraded state

On other hand, the present physical model has been proven to be an effective way to obtain the cell impedance at different frequencies and currents, that ensure enough sensitivity to all model parameters. Every cell impedance have been characterised with a reduced set of 7 parameters. Nevertheless, the identification of gas properties parameters need further measurements, particularly at high current (40-50A) where their sensitivity increases. Futures works will be run in this way.

References

Buaud, F., Lelandais, D. and Auvity, B, 2008. Evidence of a non-dimensional parameter controlling the flooding of PEMFC stack. International Journal of Hydrogen Energy, 33(11), pp.2765–2773.

Chevalier S, et al., Multiphysics DC and AC models of a PEMFC for the detection of degraded cell parameters, International Journal of Hydrogen Energy (2013)

Eikerling, M. and Kornyshev, A.., 1999. Electrochemical impedance of the cathode catalyst layer in polymer electrolyte fuel cells. Journal of Electroanalytical Chemistry, 475(2), pp.107–123.

Fouquet, N. et al., 2006. Model based PEM fuel cell state-of-health monitoring via ac impedance measurements. Journal of Power Sources, 159(2), pp.905–913.

Gerteisen, D. et al., 2011. Spatially Resolved Voltage, Current and Electrochemical Impedance Spectroscopy Measurements. Fuel Cells, 11(2), pp.339–349.

Rodat, S. et al., 2009. EIS measurements in the diagnosis of the environment within a PEMFC stack. Journal of Applied Electrochemistry, 40(5), pp.911–920.

Schmittinger, W. and Vahidi, A., 2008. A review of the main parameters influencing long-term performance and durability of PEM fuel cells. Journal of Power Sources, 180(1), pp.1–14.

Springer, T.E., 1996. Characterization of Polymer Electrolyte Fuel Cells Using AC Impedance Spectroscopy. Journal of The Electrochemical Society, 143(2), p.587.

Yuan, X. et al., 2007. AC impedance technique in PEM fuel cell diagnosis. A review. International Journal of Hydrogen Energy, 32(17), pp.4365–4380.

Ziogou C., Voutetakis S., Papadopoulou s. and Georgiadis M., (2010), Dynamic modelling and experimental validation of a PEM fuel cell system, Chemical Engineering Transactions, 21, 565-570